Radiotracers for SPECT imaging: current scenario and future prospects

By S. Adak[1,*], R. Bhalla[2], K. K. Vijaya Raj[1], S. Mandal[1], R. Pickett[2] and S. K. Luthra[2]

[1] GE Healthcare Medical Diagnostics, John F Welch Technology Center, Bangalore, India 560066
[2] GE Healthcare Medical Diagnostics, The Grove Centre, White Lion Road, Amersham, HP7 9LL, UK

Summary. Single photon emission computed tomography (SPECT) has been the cornerstone of nuclear medicine and today it is widely used to detect molecular changes in cardiovascular, neurological and oncological diseases. While SPECT has been available since the 1980s, advances in instrumentation hardware, software and the availability of new radiotracers that are creating a revival in SPECT imaging are reviewed in this paper.

The biggest change in the last decade has been the fusion of CT with SPECT, which has improved attenuation correction and image quality. Advances in collimator design, replacement of sodium iodide crystals in the detectors with cadmium zinc telluride (CZT) detectors as well as advances in software and reconstruction algorithms have all helped to retain SPECT as a much needed and used technology.

Today, a wide spectrum of radiotracers is available for use in cardiovascular, neurology and oncology applications. The development of several radiotracers for neurological disorders is briefly described in this review, including [^{123}I]FP-CIT (DaTSCAN™) available for Parkinson's disease. In cardiology, while technetium-99m labeled tetrofosmin and technetium-99m labeled sestamibi have been well known for myocardial perfusion imaging, we describe a recently completed multicenter clinical study on the use of [^{123}I]*m*IBG (AdreView™) for imaging in chronic heart failure patients. For oncology, while bone scanning has been prevalent, newer radiotracers that target cancer mechanisms are being developed. Technetium-99m labeled RGD peptides have been reported in the literature that can be used for imaging angiogenesis, while technetium-99m labeled duramycin has been used to image apoptosis.

While PET/CT is considered to be the more advanced technology particularly for oncology applications, SPECT continues to be the modality of choice and the workhorse in many hospitals and nuclear medicine centers. The cost of SPECT instruments also makes them more attractive in developing countries where the cost of a scan is still prohibitive for many patients.

1. Introduction to molecular imaging

There are two major molecular imaging modalities which are used in nuclear medicine today, namely single photon emission computed tomography (SPECT or less commonly known as SPET) and positron emission tomography (PET). Both techniques use radiolabeled molecules to probe molecular processes that can be visualized, quantified and tracked over time, thus allowing the discrimination of healthy from diseased tissue with a high degree of confidence. The imaging agents use target-specific biological processes associated with the disease being assessed both at the cellular and subcellular levels within living organisms. The impact of molecular imaging has been on greater understanding of integrative biology, earlier detection and characterization of disease, and evaluation of treatment in human subjects [1–3]. Additionally, the power of these techniques has resulted in better estimation of disease staging [4, 5] and has also aided drug development programmes [6, 7].

Out of the two techniques, SPECT is the most established modality and standard imaging procedures have been widely available in most hospitals since the early 1990s. Although SPECT has been used to investigate many applications in neurology and oncology, the majority of SPECT procedures are performed in the field of cardiology, particularly in the assessment of coronary perfusion and myocardial viability [8].

The radiotracers used in SPECT emit gamma rays, as opposed to PET isotopes which are positron emitters, such as, ^{11}C ($T_{1/2} = 20.4$ min), ^{18}F ($T_{1/2} = 110$ min). The SPECT radiotracers have relatively long half-lives from a few hours to a few days (^{99m}Tc $T_{1/2} = 6.0$ h; ^{111}In $T_{1/2} = 67.3$ h; ^{123}I $T_{1/2} = 13.3$ h; ^{201}Tl $T_{1/2} = 72.9$ h) and their use can be tailored to the specific application being investigated. As well as development of imaging agents [9, 10], there has been an even greater emphasis on the development of new SPECT imaging systems with increased sensitivity and improve image quality and resolution [11]. It is anticipated that advancement in both directions will greatly influence the future of molecular medicine.

In most countries today, the number of SPECT cameras exceeds the number of PET systems and for developing nations like India and China, SPECT availability is as high as 4–5 times more than PET. As advances in PET and hybrid PET imaging (PET/CT or PET/MRI) come into wider use, it is natural to ask if the modality of the future will be dominated by PET or will there be a role for SPECT imaging as well. This article reviews SPECT radiotracers available and

---

*Author for correspondence (E-mail: sudeshna.adak@ge.com).

in development today that are critical to the continuing role of SPECT in diagnosis and therapy monitoring.

2. Role of SPECT

Since the first use of the Anger camera in the 1950s and the advent of the modern SPECT camera in the 1970s, SPECT imaging has become widely accepted in the diagnosis, monitoring and evaluation of diseases. Some of the advances that have fuelled this growth in the last couple of decades have been: (1) Improvements in SPECT collimators from simple parallel to pin hole and fan beam collimators; (2) Development from single-head to multihead cameras; (3) Improvements in detectors to use cadmium zinc telluride (CZT) that allow direct conversion of gamma rays into electrical signals and have higher intrinsic resolution; (4) Hybrid SPECT/CT systems that have improved image quality; (5) New SPECT radiotracers that target disease mechanisms for more sensitive and specific detection.

2.1 Image quality

Image quality in SPECT is determined by attenuation, scatter, spatial and energy resolution and statistical fluctuations (image noise) and contrast (target to background ratio).

The integration of CT with SPECT has allowed for attenuation correction that has improved the image quality, and the CT also provides fair anatomical images [12]. The CT image is acquired prior to the SPECT image and produces an attenuation map of the spatial distribution of the attenuation coefficients. However, in a SPECT/CT system, patient movement between the two acquisitions can lead to incorrect attenuation correction and misregistration.

Scatter in SPECT images can reduce image contrast, lead to inaccurate quantification and even for artifacts to be seen in a region of no activity or outside the patient. Various scatter correction algorithms have been reviewed previously [13], including scatter model based correction strategies and strategies based on iterative reconstruction algorithms.

Image quality is a tradeoff between resolution, sensitivity, field of view (FOV) and detector area [14]. While overall image quality in PET is considered superior for many applications, the new advances in instrumentation and software have made SPECT highly valued.

2.2 PET *vs.* SPECT

SPECT spatial resolution stands today at ~ 10 mm while PET spatial resolution is at ~ 5 mm. Despite the challenges of spatial resolution in SPECT, a comparison of PET *vs.* SPECT studies shows that SPECT continues to be a modality of choice in various clinical applications, especially in cardiology.

2.2.1 Cardiology PET *vs.* SPECT

SPECT is well established as the modality of choice in myocardial perfusion imaging. The clinical guidelines on use of radionuclides from the American College of Cardiology and the American Heart Association [15] report that average

sensitivity is 87% for detecting angiographically significant coronary artery disease, while average specificity is 73%. The guidelines also recommend the use of [18F]FDG PET to assess myocardial viability.

2.2.2 Oncology PET *vs.* SPECT

For oncology applications, PET is the modality of choice with multiple radiotracers being used for imaging ([18F]FDG for glucose metabolism, [18F]FLT for cell proliferation, 18F labeled RGD for angiogenesis, [18F]ethylcholine for prostate, *etc.*). However, SPECT continues to be the modality of choice in bone scintigraphy. In a study on the use of [18F]FDG PET *vs.* SPECT (using 99mTc-HMDP) in detecting bone metastases from breast cancer [16], a lesion-by-lesion analysis in 15 patients showed that SPECT was more sensitive (85%) compared to PET (17%) and the overall accuracy of SPECT was higher (96%) compared to PET (85%).

2.2.3 Neurology PET *vs.* SPECT

It has been well established that 99mTc-hexamethylpropyleneamine oxime (99mTc-HMPAO) SPECT and [18F]FDG PET can be used to detect cerebral perfusion and metabolic abnormalities seen in Alzheimer's disease. In a direct comparison of spatially normalized PET and SPECT in Alzheimer's [17], it was shown that there was a high correlation in the number of abnormal voxels seen in PET and SPECT in specific regions of the brain (temporoparietal and posterior cingulate association cortices). For neurological disorders like Alzheimer's and Parkinson's, specific radiotracers that target the disease mechanism ([18F]PIB to detect amyloid plaques, [123I]FP-CIT (ioflupane) to detect Parkinson's described later in this article) will impact the clinical workflow. For SPECT to be useful in neurology, 123I is preferred for improved blood brain barrier penetration as compared to the larger 99mTc chelated molecules.

2.2.4 SPECT – the right choice?

In a commentary on the future of nuclear medicine [18], the authors argue that while SPECT technology faces competition from PET, the role of SPECT in clinical investigations will continue. The wide availability of SPECT scanners, comparatively simpler and less expensive infrastructure requirements, and lower cost of SPECT scans will continue to drive the use of SPECT across the world.

3. Radiolabeling

3.1 Technetium-99m labeling

There are several reviews on technetium published [19–21], and we refer the readers to them for a detailed review of this element. In this section, we provide a brief summary highlighting some of the key aspects in the design of radiotracers based on technetium-99m.

Technetium-99 exists commonly as two isomers: 99gTc and 99mTc. The longer-lived 99gTc is used to study the coordination chemistry of technetium and verify the structures of compounds of technetium. 99mTc, its most widely
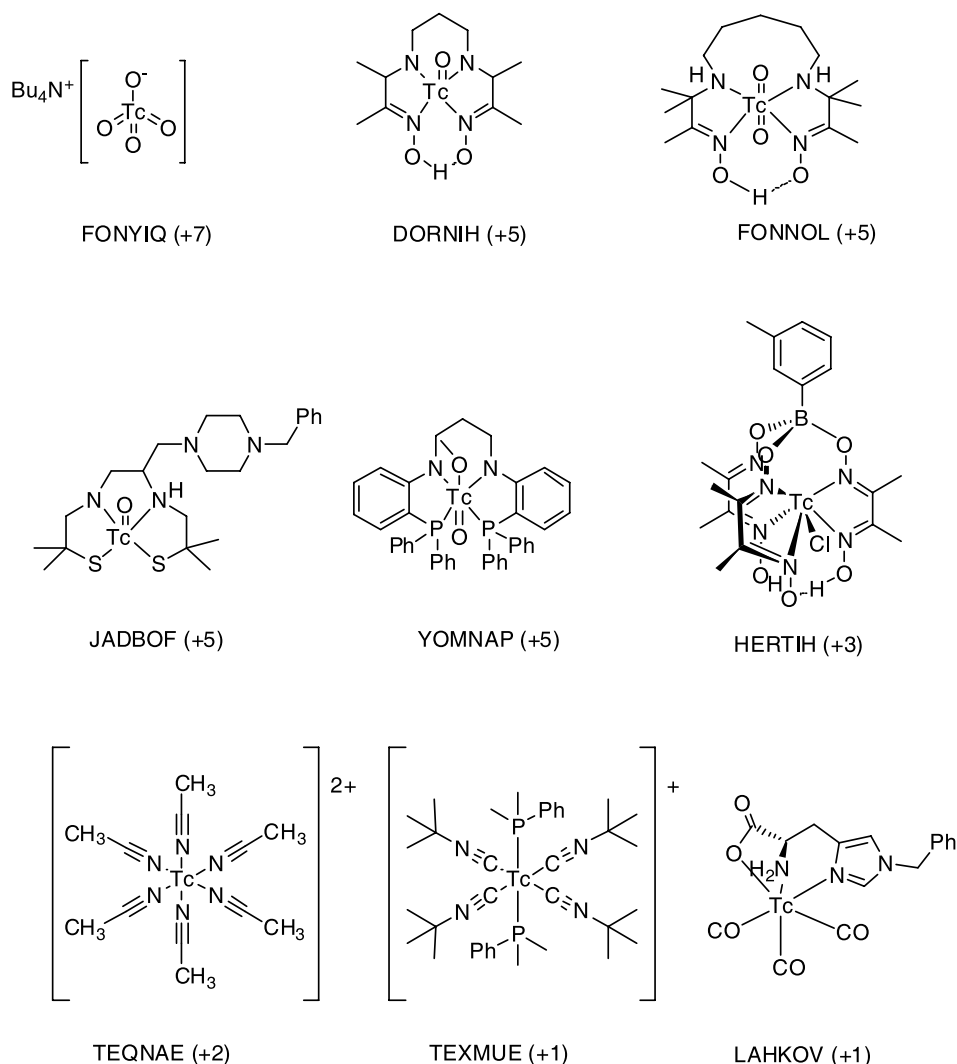
Fig. 1. Snapshot of technetium complexes, which have been characterized by X-ray crystallography. Cambridge Crystallographic Reference numbers are included under each complex and the oxidation state of the technetium ion is presented in parentheses.

studied isotope, has become the mainstay of diagnostic nuclear medicine. ^{99m}Tc (as [^{99m}Tc]pertechnetate) is produced by the decay of ^{99}Mo, and is available commercially *via* elution (with 0.9% saline) of alumina columns that have ^{99}Mo adsorbed on them.

The synthesis of a ^{99m}Tc radiotracer typically involves three components:

I.   Pertechnetate (^{99m}TcO$_4^-$).
II. A reducing agent (*e.g.* Sn(II), Fe(II), Cu(I), as well as non-metallic reducing agents such as dithionite, borohydride).
III. and a chelator.

The design of chelators is critical in the development of technetium radiotracers and consequently there has been significant work performed synthesizing chelators which rapidly complex with technetium to form stable complexes. Understanding the coordination chemistry of technetium is therefore critical in the development of new chelators.

In spite of the challenges of handling ^{99g}Tc (a long-lived isotope requiring dedicated chemistry laboratories) a large number of technetium complexes have been reported, many of which have been characterized by crystallography (there are greater than 700 X-ray structures of technetium complexes on the Cambridge Crystallographic Database) [22].

Whilst the chemistry of technetium is dominated by the +5 oxidation state, it is clearly evident that stable technetium complexes with a variety of other oxidation states can be prepared. Different chelators stabilize different oxidation states and this has been used in developing technetium complexes with differing physicochemical properties (*e.g.* lipophilicities and charge of the complex). Fig. 1 displays a snapshot of some of the technetium complexes, which have been characterized by X-ray crystallography, highlighting the variety of coordination environments, which can be tolerated by technetium. The Cambridge Crystallographic Reference numbers are included under each complex and coordinates are available (as a cif file) from ccdc.cam.ac.uk.

3.2 Iodine-123 labeling

Whilst there are many isotopes of iodine, only one stable isotope, iodine-127 is found in nature. Four radioisotopes (^{123}I, ^{124}I, ^{125}I, ^{131}I) have been widely used for labeling both small and large molecules. Whilst this section focuses on iodine-123, the chemistry strategies for the other isotopes are essentially the same [23].

Iodine-123 is produced at a cyclotron and there are several different production routes, but typically it is formed
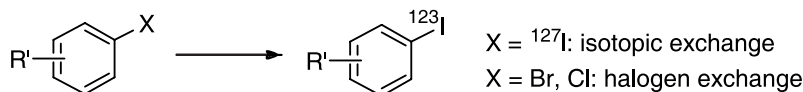
X = ^{127}I: isotopic exchange
X = Br, Cl: halogen exchange

Fig. 2. Nucleophilic substitution to label with ^{123}I.

using highly enriched ^{124}Xe as a target. Typically it is supplied as Na^{123}I in a 0.1 M NaOH solution. The labeling of compounds with iodine-123 can be achieved either by nucleophilic or electrophilic substitution.

3.2.1 Nucleophilic substitution

The simplest way to introduce iodine-123 into a small molecule is *via* isotopic exchange (Fig. 2). This results in regiospecific substitution (usually catalyzed by copper or gold) generally with good radiochemical yields. Purification of the radiolabeled product tends to be simple, but since the iodine-127 precursor cannot be chemically separated from the radiolabeled derivative, lower specific activities are achieved. Higher specific activities can be achieved, but purification is required (typically HPLC). Similar halogen-exchange reactions can be achieved with high regiospecific substitution from the corresponding chlorine or bromine containing compounds – however radiochemical yields tend to be lower.

3.2.2 Electrophilic substitution

Electrophilic iodination chemistry is the predominant approach for the introduction of iodine-123 into biomolecules. This requires the oxidation of iodide, which is easily achieved since the oxidizing potential of iodide is low and this allows for the direct formation of an electrophilic species in which the iodine is oxidized to I$^+$. A number of oxidizing agents have been used in iodine-123 chemistry for the oxidation of iodide to I$^+$ (peracids, iodine monohalide, N-chloroamides, iodogen) and these are described elsewhere [23].

Iodo-deprotonation

Iodo-deprotonation is generally limited to arenes which are activated for electrophilic substitution (Fig. 3). The presence of tyrosine residues in peptides means that this may be a simple and fast approach to label the compound. Whilst this method is relatively simple, if the compound to be labeled is asymmetrical, a mixture of compounds may be formed [24].
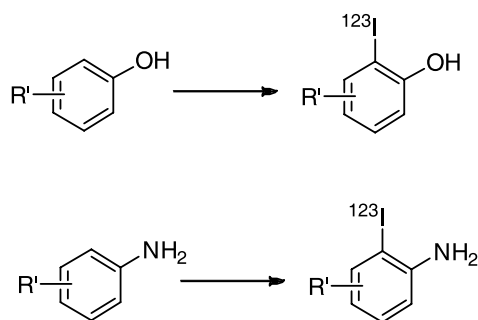

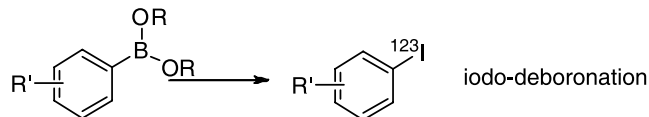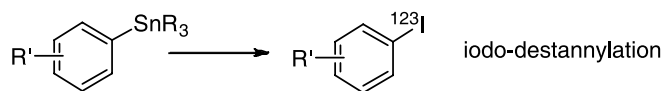**Fig. 3.** Electrophilic substitution (iodo-deprotonation).

iodo-destannylation

iodo-deboronation

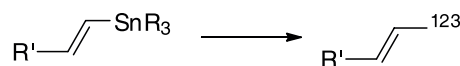**Fig. 4.** Iodo-destannylation and iodo-deboronation.

Fig. 5. Iodo-destannylation with retention of configuration across a double bond.

Site specific electrophilic substitutions

Two strategies for labeling compounds with high regiospecificity are shown in Fig. 4. Iodo-destannylation and iodo-deboronation have become popular since they generally result in good radiochemical yields and can often be performed at room temperature [25, 26].

This high selectivity using trilalkyltin derivatives facilitates the introduction of the iodine-123 to label alkenes with retention of configuration across the double bond [27] as seen in Fig. 5.

Indirect labeling

Methods for labeling biomolecules such as peptides should, in general, be mild and rapid affording high radiochemical yields. However, whilst the previous methods afford simple and rapid labeling, the presence of oxidizing agents required to generate "I$^+$" may not make them suitable for labeling biomolecules (which are sensitive to oxidizing agents). To overcome this obstacle, it is possible to pre-label a small molecular weight synthon with iodine-123 and then to perform the coupling to the sensitive biomolecule using milder (non-oxidizing) conditions. Fig. 6 depicts the formation of a radioiodinated active ester, which is coupled on to an amine residue (*e.g.* lysine) of a biomolecule.

4. SPECT radiotracers for neurology

SPECT can be used non-invasively to indirectly monitor changes in neurotransmitter concentration, provided that (i), a radiotracer specific and selective for the system of interest is available, and (ii), the radiotracer binds to the same site as the endogenous ligand, or neurotransmitter. Over the last 15 years, many studies have demonstrated the use of SPECT to non-invasively measure acute changes in neurotransmitter levels *in vivo* [28], initially assuming a direct competition between the radiotracer and the endogenous neurotransmitter at the binding site. The basic concept of the
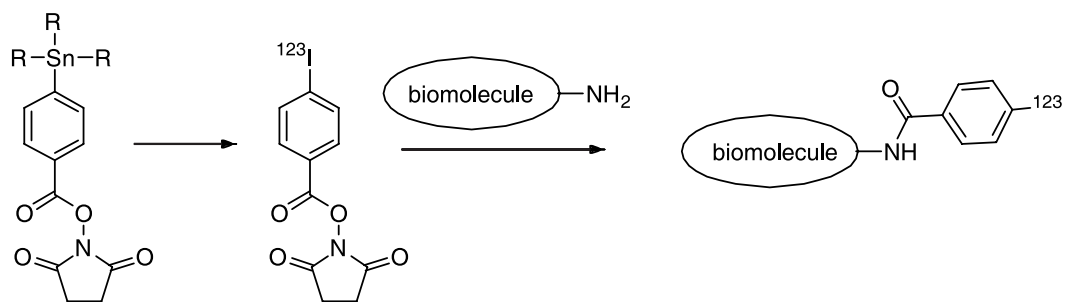
Fig. 6. Labeling peptides with iodinated synthons.

Table 1. Common SPECT radiotracers and radiotracers available for neurology.

Target	SPECT radiotracer/ligand
Regional cerebral perfusion	^{99m}Tc-bicisate (ECD, Neurolite™), ^{99m}Tc-exametazime (HMPAO, Ceretec™), [^{123}I]iodoamphetamine ([^{123}I]IMP)
Cerebrospinal fluid kinetics	^{111}In-Pentetate
Phosphatidylserine – dementia	^{99m}Tc-HYNIC – annexin V
Dopamine D2, D3 receptors	[^{123}I]iodobenzamide (IBZM), [^{123}I]epidepride
Dopamine reuptake transporter	[^{123}I]ioflupane, [^{123}I]altropane, ^{99m}Tc-TRODAT
Peripheral benzodiazepine receptor (PBR)	[^{123}I]PK11195
Amyloid	[^{123}I]IMPY
Serotonin teuptake transporter (SERT)	[^{123}I]IDAM, [$^{'123}$I]ADAM
GABA receptor	[^{123}I]iomazenil

"occupancy model" predicts that uptake/retention of tracer levels of a specific radioligand at the site of its receptor will be inversely related to the local concentration of the competing neurotransmitter. However, because the status of the receptor (availability due to up- or down-regulation, internalization, altered affinity states) may also change with the stimulus leading to the change in the neurotransmitter concentration, each combination of receptor, radioligand, neurotransmitter and stimulus must be fully understood before such determinations can be made routinely. Such a discussion is unfortunately beyond the scope of this general review of radioligands for SPECT imaging.

An early challenge of the SPECT modality was to design a radiotracer that crossed the intact blood–brain-barrier (BBB) to permit imaging of the brain. Previously, hydrophilic radiotracers like ^{99m}Tc-DTPA (pentetate) or [^{99m}Tc]pertechnetate, which would normally be excluded by the blood brain barrier (BBB), were used to detect areas where the BBB had been compromised (for example, at the site of an intracranial tumor). More recently, lipophilic molecules and complexes have been designed that can cross the BBB, either by passive diffusion or by facilitated transport. Once inside the brain, various targeting or retention mechanisms can be employed to allow selective retention at the diagnostic target while allowing background clearance of unbound radioactivity.

The increase in neurological applications for SPECT over the last decade has been greatly aided by the signifi-

cant improvement in data acquisition (hardware technology), data quantification (model-based methodology) and the growing number of available SPECT metabolic radiotracers and receptor-specific radiotracers. Table 1 lists the more common SPECT radiotracers/ligands and their intended targets in clinical neurology, with structures shown in Fig. 7. A more detailed review can be found in [29].

4.1 Cerebrovascular diseases

In the early 1980s, N-isopropyliodoamphetamine radiolabeled with iodine-123 was introduced as one of the first radiotracers that crossed the BBB and was retained approximately in proportion to regional cerebral perfusion. Retention was thought to be due to conversion to a less lipophilic form of the molecule, possibly by N-demethylation, within the brain. The images were however degraded as a result of the slow diffusion of radioactivity from the lungs, which took up a large proportion of the administered activity immediately after injection. Subsequently, complexes of technetium were developed *e.g.*, ^{99m}Tc-exametazime (HMPAO, Ceretec™) and ^{99m}Tc-bicisate (Neurolite™), which behave in a similar manner (passive uptake followed by intracerebral conversion to a less lipophilic, less diffusible form and subsequently trapped intracellularly, in proportion to the blood flow). Although assessment of cerebral blood flow using SPECT radiotracers has provided clinical diagnostic information, the SPECT technique does not
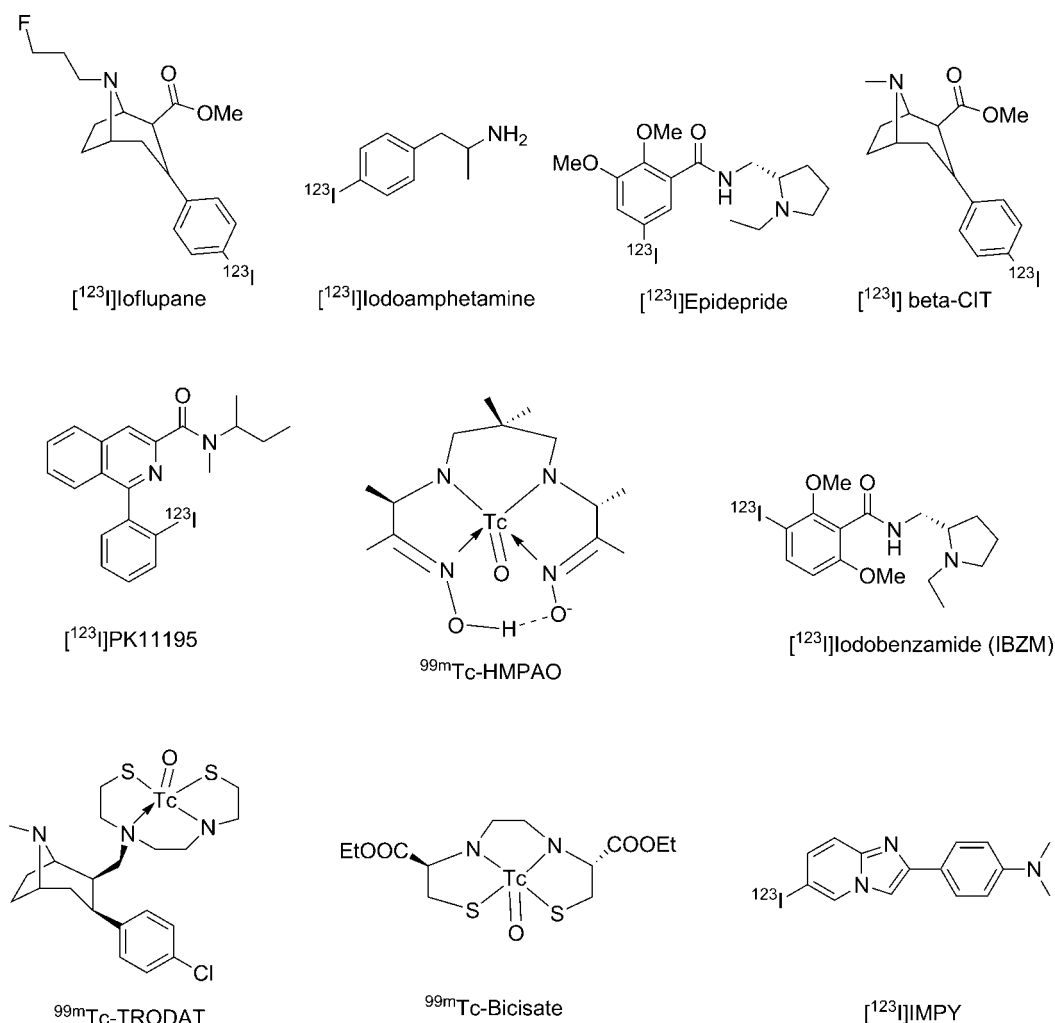
Fig. 7. Common SPECT radiotracers for neurology applications.

provide high resolution images and the data are not optimal for the quantitative estimation of the rate of cerebral blood flow and perfusion. The two technetium-99m radiotracers, ^{99m}Tc-exametazime and ^{99m}Tc-bicisate, are however frequently used for the assessment of regional cerebral perfusion in neurological diseases, replacing the less convenient xenon-133 gas or solution in this role.

4.2 Alzheimer's disease (amyloid ligands)

Alzheimer's disease (AD) is the most important and common degenerative brain disorder where a person shows progressive memory loss and decrease in cognitive function. AD is characterized by the presence of abundant amyloid plaques in the brain. Thus, *in vivo* imaging agents targeting amyloid plaques might serve as suitable markers for monitoring the amyloid burden, following the disease progression and further provide indication for therapeutic intervention. Several research groups have studied biomarkers for imaging amyloid plaques in the brain [30, 31]. [^{123}I]IMPY, a modified thioflavin derivative is a novel agent displaying high binding for amyloid plaques and favorable brain uptake kinetics in rodents. Seibyl *et al.* [32] have shown that this radiotracer is a good candidate for the detection of amyloid plaques in human Alzheimer's subjects when used with SPECT.

4.3 Parkinson's disease (dopamine transporter)

Parkinson's disease is a degenerative condition characterized by tremor, hypokinesis and rigidity. Following the release of the neurotransmitter dopamine into the synapse, the dopamine is transported back into the pre-synaptic nerve terminal by a specific dopamine transporter (DAT) present on the pre-synaptic plasma membrane. Cocaine and its analogues bind to this transporter, block the reuptake of dopamine, and increase the intra-synaptic dopamine levels. A large number of radiolabeled DAT ligands have been developed based on the chemical structure of cocaine because of its relatively high affinity for the DAT. These include radiotracers such as [^{123}I]β-CIT (*N*-methyl-2β-carbomethoxy-3β-(4-iodophenyl) tropane), [^{123}I]IPT (*N*-(3-iodopropen-2-yl)-2β-carbomethoxy-3β-(4-chlorophenyl) nortropane), [^{123}I]PE2I (*N*-(3-iodoprop-(2E)-enyl)-2β-carbomethoxy-3β-(4-methylphenyl)nortropane), [^{123}I]2β-carbomethoxy-3β-(4-fluorophenyl)-*n*-(1-iodoprop-1-en-3-yl)nortropane (altropane) and [^{123}I]*N*-(3-fluoropropyl)-2β-carbomethoxy-3β-(4-iodophenyl)nortropane ([^{123}I]-FP-CIT; [^{123}I]ioflupane). [^{123}I]Ioflupane is routinely available commercially as DaTSCAN™ and is a SPECT radiotracer that binds to the pre-synaptic dopamine transporter to give images of the normal striata (Fig. 9a). In cases of striatal dopaminergic deficit (such as are seen in Parkinsons
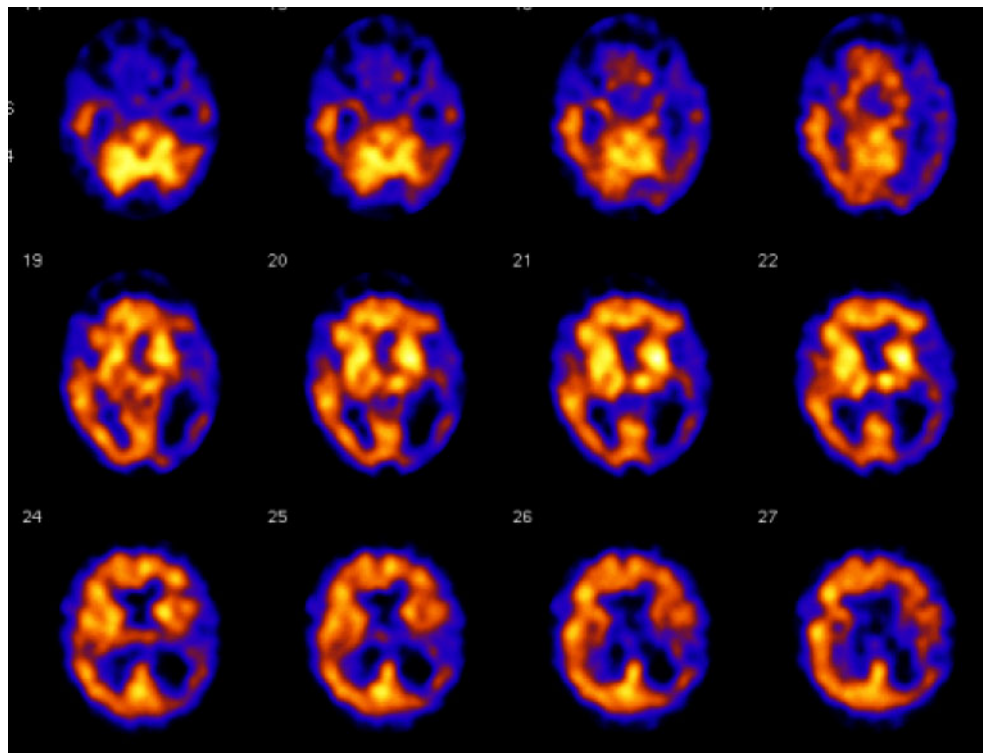
Fig. 8. Regional cerebral perfusion images obtained with Ceretec™. Note: Hypoperfused region at the bottom right of these images from a stroke patient (courtesy: GE Healthcare).
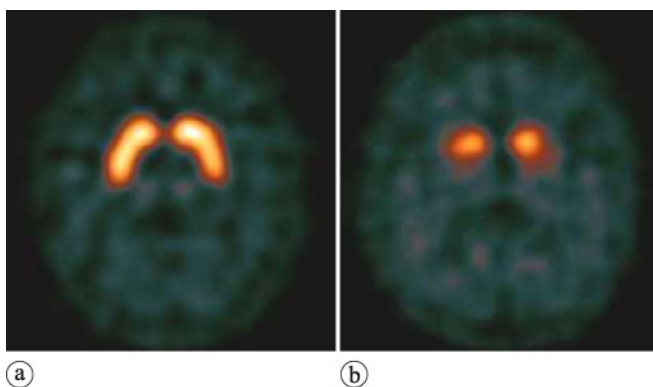

Fig. 9. DaTSCAN [123I]ioflupane images of human striata. (**a**) Normal scan shows characteristic comma shape. (**b**) Striatal dopaminergic deficit seen where comma shape degrades.

disease and Dementia with Lewy Bodies) the characteristic symmetrical "comma" shape of the two striata usually becomes asymmetric and/or degraded to the shape of a "full stop" (Fig. 9b).

The technetium-99m labeled TRODAT (or tropantiol), like ioflupane, is a tropane analogue of cocaine and similarly, binds to the dopamine transporter. On the basis of a N2S2 chelating agent, known as bisaminoethanethiol (BAT), ^{99m}Tc-TRODAT-1 was developed for SPECT imaging studies [33]. The brain uptake of this technetium-99m complex is however lower than that of [123I]Ioflupane, so the convenience of the "cold kit" presentation is balanced by the reduced image quality.

4.4 Dopamine receptors

D_1 and D_2 receptors are highly concentrated in the striatum and a number of antagonist radiotracers have been in-

vestigated. This extensive research in this field is in part due to the successful discovery that the binding of the D_2 receptor radiotracer, [123I]IBZM, is particularly sensitive to changes in dopamine levels [34]. [123I]IBZM has been shown to be useful for semi-quantitative imaging of striatal D_2 dopamine receptors and for estimating their blockade by neuroleptics. Thus, it may improve drug monitoring in psychiatric patients [35]. The availability of iodine-123-labeled post-synaptic, and technetium-99m-labeled presynaptic dopaminergic radiotracers, affords the possibility of dual-isotope studies of this important region of the brain.

4.5 Serotonin transporter

^{123}I-labeled IDAM and ADAM are potent inhibitors of the serotonin reuptake transporter (SERT), based on the parent compound, a phenylthiophenyl derivative known as 403U76. They possess high selectivity and affinity for SERT over norepinephrine and dopamine transporter binding sites. According to the initial human studies, [123I]ADAM localizes in the hypothalamus, a region known to have high SERT concentration. [123I]ADAM is superior to [123I]IDAM as a SPECT imaging agent for SERT in the brain [36].

4.6 Neuroinflammation

Peripheral benzodiazepine binding sites (PBBS) are present at low levels in the normal brain. These sites are highly expressed *in vivo* by activated microglia, which are associated with CNS inflammation in a wide range of pathologies. In combination with MRI, to aid with anatomical definition, SPECT imaging using the PBBS-selective ligand, [123I]PK11195 provides a generic indicator of active disease in the brain and, to date, has been used in clinical studies of stroke, multiple sclerosis, dementia, Parkinson's disease,

Huntington's chorea, epilepsy and schizophrenia [37]. However, this ligand, along with a ^{11}C-labeled version for PET, suffers from poor brain uptake. The radiotracers most widely used for imaging central benzodiazepine-binding sites are based on the antagonist, Ro-15-1788 (flumazenil). The ^{123}I labeled analogue, Iomazenil, binds mainly to an $\alpha 1$ subtype of the GABA$_A$ receptors in the medial occipital cortex, followed by other cortical areas.

The neuropharmacological data obtained from receptor-specific SPECT studies can additionally help in increasing knowledge about potential therapeutic targets for novel pharmaceutical agents by determining their dose/occupancy profile. This can be done using the radiolabeled drug under investigation or by monitoring its effects on the binding of an established radiotracer. In using the radiolabeled drug, regional brain pharmacokinetic data are obtained within a very short time frame. Alternatively, by quantifying the pharmacology and the effects of an experimental drug on the specific binding of an established radiotracer, we can develop an understanding of the relationships between the drug's efficacy, plasma concentration and receptor occupancy. As the number of PET/SPECT centers grows, applications of the use in clinical neurology will increase for early and/or presymptomatic diagnosis of diseases. As more target-specific radiotracers and ligands are developed, the use of these in clinical research and drug development will help determine optimal drug dosing regimes and elucidate the down-stream effect of drug actions.

5. SPECT radiotracers for cardiovascular disease

The current focus of cardiovascular medicine is on early detection and prevention of disease. Worldwide, coronary artery disease (CAD) is the single most important cause of morbidity and mortality. The most common SPECT radiotracers used in cardiovascular imaging are shown in Fig. 10.

5.1 Myocardial perfusion imaging

Radionuclide myocardial perfusion imaging during exercise or pharmacological stress and at rest is widely used for diagnosis of ischemic heart disease [38, 39]. The underlying principle is that under conditions of stress, the diseased myocardium receives less blood flow than normal myocardium. Specific radiotracers can be administered that indicate the reduced blood flow *e.g.* [99mTc]-tetrofosmin (Myoview, GE Healthcare), [99mTc]-sestamibi (Cardiolite, Bristol-Myers Squibb).

5.1.1 Myoview™ (technetium ([99mTc]) tetrofosmin)

Imaging with Myoview™ is useful in the diagnosis and localization of regions of reversible myocardial ischemia in the presence or absence of infarction. Its characteristic high target to background ratio provides clear images [40] indicating regions of low perfusion. It also demonstrates good sensitivity, specificity and diagnostic accuracy.

The structural formula of Myoview™ is shown in Fig. 10 and the radiotracer technetium-99m is chelated by two 1,2-bis[di-(2-ethoxyethyl)phosphino] ethane ligands.

5.1.2 Cardiolite (technetium ([99mTc]) sestamibi)

It is a lipophilic monocationic complex of technetium(I) with the ligand methoxyisobutylisonitrile (MIBI) [41]. When injected intravenously into a patient, it distributes in the myocardium proportionally to the myocardial blood flow. It was the first successful [99mTc]-labeled substitute for [^{201}Tl]thallous chloride for myocardial perfusion imaging and diagnosis of myocardial infarction. Although it shares with Tl$^+$ the positive charge, supposed to be a prerequisite for transport by Na$^+$/K$^+$-ATPase (Na$^+$/K$^+$ Pump), its mechanism of uptake in myocytes has been shown to be largely different from that of Tl$^+$. This is to date the most successful and most intensively used SPECT radiotracer.

5.2 [^{123}I]*m*IBG imaging in heart failure

Metaiodobenzylguanadine (*m*IBG) or Iobenguane was developed almost 30 years ago at the University of Michigan as an imaging agent for pheochromocytoma. *m*IBG accumulates in the adrenergic nerve terminals *via* the norepinephrine transporter system. While [^{123}I]*m*IBG was originally developed for imaging adrenergic tumors, various studies in the last 30 years [42–46] have shown [^{123}I]*m*IBG to be very useful in study of the sympathetic innervations of the heart.
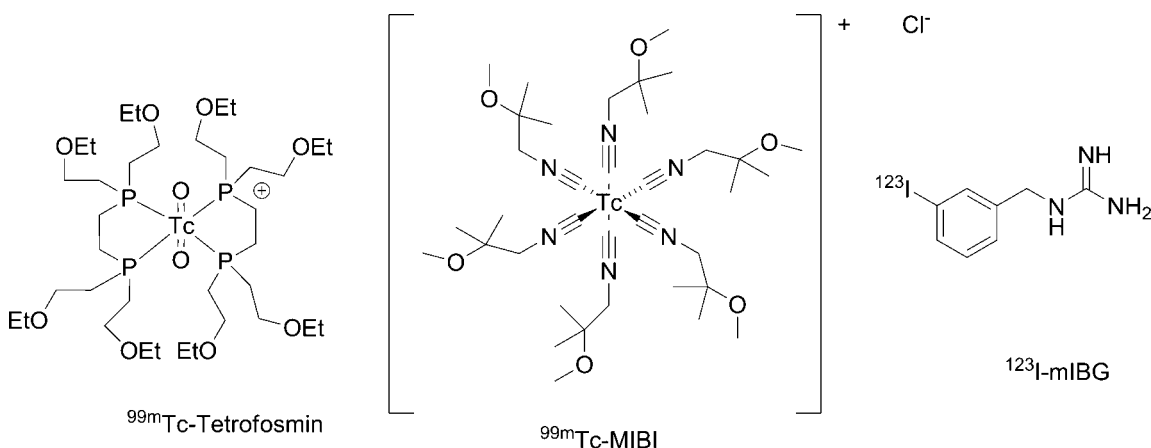

Fig. 10. Most common [99mTc] radiotracers used in cardiovascular imaging.

A review of the literature [47] on [^{123}I]mIBG showed that over 30% of publications have focused on the use of mIBG in cardiac applications, especially from Japan where [^{123}I]mIBG was available for use. Semi-quantitative parameters used to measure mIBG uptake include early and late heart-to-mediastinum (H/M) ratios and myocardial washout. While there have been many clinical studies that show that H/M ratios and myocardial washout could have prognostic significance, some clinical studies have failed to show any prognostic significance of these measures. However, a recent meta-analysis [48] and the results of the large multicenter ADMIRE-HF (AdreView Myocardial Imaging for Risk Evaluation in Heart Failure) [49] have provided conclusive results on the benefits of using [^{123}I]mIBG.

The meta-analysis [48] used 18 studies with a total of 1755 patients reported in the literature between 1999 and 2005 (except one study from 1992). As there was significant heterogeneity, the 3 best quality studies were used for a subset meta-analysis and the pooled hazard ratio for a cardiac event and late H/M was 1.98 ($p < 0.001$). Myocardial washout was a significant prognostic factor in predicting cardiac death (hazard ratio = 1.72, $p = 0.006$) and cardiac events (hazard ratio = 1.08, $p < 0.001$). The ADMIRE-HF was a prospective study of 961 heart failure patients followed up over 2 years that evaluated the prognostic value of [^{123}I]mIBG in predicting cardiac events. The hazard ratio for H/M was 0.40 ($p < 0.001$); the significant contributors to the multivariable model were H/M, LVEF, B-type natriuretic peptide, and New York Heart Association functional class.

In cardiac [^{123}I]mIBG imaging, it has been well validated that the choice of collimator can impact the image quality and subsequent uptake parameters like H/M and washout [50]. It is preferred to use a medium energy collimator that prevents septal penetration of the high energy photons that come from ^{123}I (2.87% photons have an energy more than 400 keV). This can improve the image quality by reducing scatter and thus improve the quantitative accuracy of H/M ratios.

6. SPECT and oncology

Bone scanning is clinically important for patients in whom detection of cancer that has spread to the bone would result in treatment changes. This includes patients with breast, prostate and lung cancer. ^{99m}Tc-MDP planar bone scanning or [^{18}F]FDG PET/CT have been routinely used to scan bone metastases [51, 52]. Although whole body SPECT imaging with ^{99m}Tc-MDP is more sensitive than planar bone imaging, routine clinical whole body SPECT imaging is not performed because of the long image acquisition time required. The past decade has seen the invention of many alternatives to [^{18}F]FDG that target specific aspects of tumor biology. These targets include molecular biomarkers such as growth factor receptors, protein kinases, specific receptor over-expression or biological events such as angiogenesis, apoptosis, hypoxia and tumor proliferation. Many focused efforts were reported for developing SPECT radiotracers for angiogenesis and apoptosis and the most promising radiotracers are discussed here.

6.1 SPECT imaging of angiogenesis

Angiogenesis is the formation of new blood vessels through capillary sprouting from pre-existing vasculature. Angiogenesis plays a key role in the growth and metastatic potential of solid tumors [53, 54]. Tumor growth beyond a 1–2 mm^3 volume requires an independent vasculature for the cellular supply of oxygen and nutrients and removal of waste products [55]. Consequently, tumors that outgrow their existing blood supply frequently display oxygen deficiency (hypoxia) that can trigger the secretion of various pro-angiogenic growth factors, such as, vascular endothelial growth factors (VEGFs) for initiating new blood vessel growth [53]. Binding of VEGFs to the VEGF family of receptors (VEGFR) initiates a signaling cascade that promotes the proliferation, migration and survival of endothelial cells, ultimately leading to angiogenesis [56, 57]. VEGF radiolabeled with ^{64}Cu has been reported for small animal PET imaging of VEGF receptor expression *in vivo* [58, 59].

An indirect and better approach to angiogenesis imaging has focused on radiotracers targeting the $\alpha_v\beta_3$ class of cell adhesion molecule integrins [60]. Integrin $\alpha_v\beta_3$ receptors are significantly upregulated in endothelial cells during angiogenesis but not in mature vessels or non-neoplastic epithelium [61–63]. Integrin $\alpha_v\beta_3$ is also expressed in a variety of tumor cells, including melanoma, late-stage glioblastoma, ovarian, breast and prostate cancer [64]. The ability to visualize and quantify integrin $\alpha_v\beta_3$ expression *in vivo* would allow for appropriate selection of patients for anti-integrin treatment and also for treatment monitoring in such patients.

Integrins are known to bind to peptides with exposed arginine-glycine-aspartate (RGD) sequence and labeling of the $\alpha_v\beta_3$ integrin with ^{99m}Tc-RGD peptide provides a potential tool for imaging angiogenesis [65, 66]. It has been shown in a previous study in females with histologically proven breast cancer that the detection of malignant breast tumors is feasible and efficient by scintigraphic imaging with ^{99m}Tc-RGD peptide [67, 68]. Fig. 11 shows the structure of NC100692 (maraciclatide), the RGD peptide that has been labeled with technetium for the study in breast cancer [67].

Fig. 12 shows the characteristic annular uptake of the RGD peptide labeled with technetium-99m. As the exact role of $\alpha_v\beta_3$ in the context of angiogenesis still is a matter of debate, more information on the correlation of $\alpha_v\beta_3$ expression and other potential targets for antiangiogenic drugs, like MMPs and VEGF receptors, is needed, in order to evaluate, if imaging of $\alpha_v\beta_3$ expression really is a valid surrogate parameter for angiogenic activity. Other targets exclusively expressed on activated endothelial cells like $\alpha_5\beta_1$ might eventually be better suited for imaging of angiogenesis. Moreover, imaging of $\alpha_v\beta_3$ expression for assessment of therapeutic response or angiogenic activity will have to compete with "conventional" imaging methods of therapy response and angiogenesis, like [^{18}F]FDG PET and DCE MRI/DCE CT.

6.2 SPECT imaging for apoptosis

Apoptosis (programmed cell death) plays a critical role in the homeostasis of multicellular organisms and non-invasive
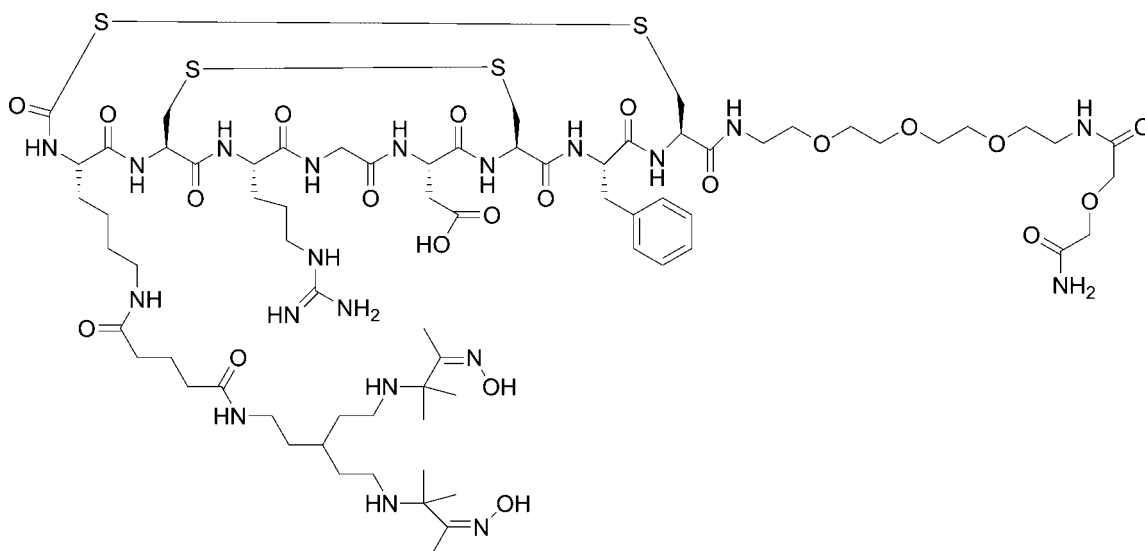
Fig. 11. Structure of the -RGD peptide, which has been labeled with technetium for a study of angiogenesis in breast cancer patients [67].
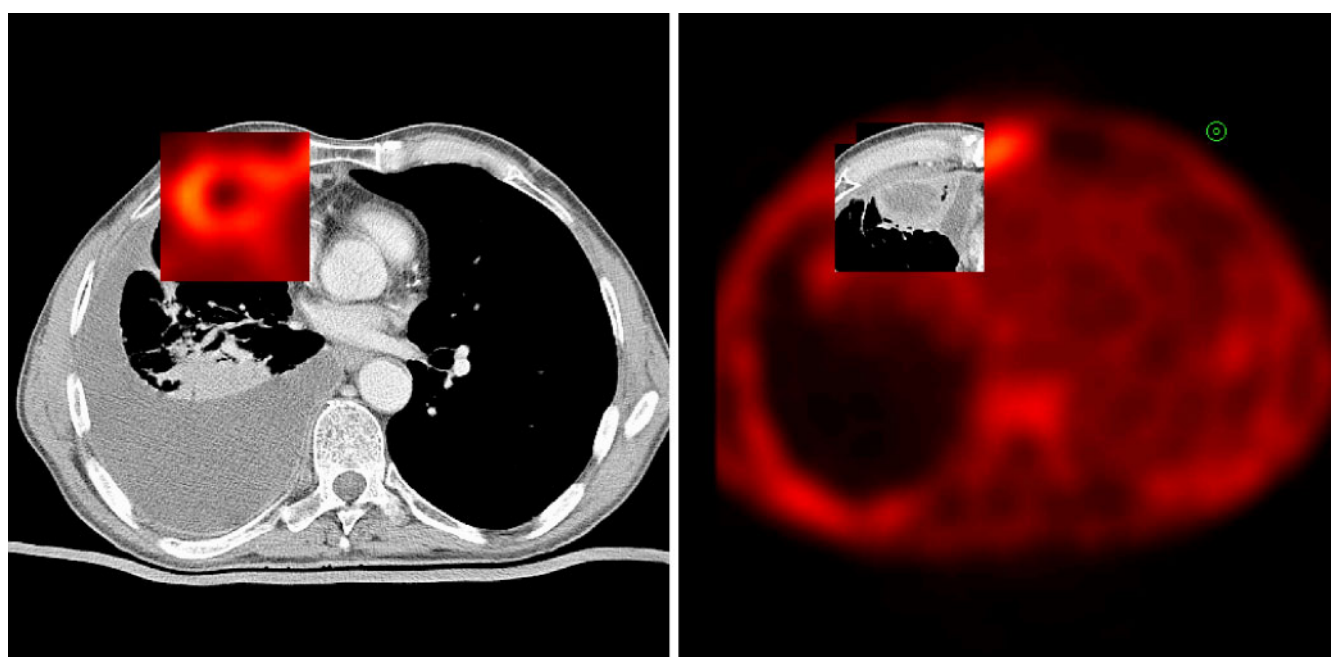

Fig. 12. ^{99m}Tc-maraciclatide study showing SPECT/CT registration. Primary cancer seen in right lung (note annular uptake and necrotic center). Right lung also shows pulmonary effusion.

in vivo imaging of cell death has important clinical diagnostic and prognostic value. During apoptosis, it is well documented that cell surface exposure of phospholipids such as phosphatidylserine (PS) and phosphatidylethanolamine (PE) occurs [69]. In viable cells these phospholipids are almost exclusively found on the inner leaflet of the plasma membrane and this asymmetry is maintained by active energy dependent enzymes and translocases [70]. However, during apoptosis the mechanisms that maintain this asymmetry are lost and the redistribution of phospholipids is actively facilitated by scramblases [71]. Therefore, the externalisation of PE and PS is a universal marker for those cells that are committed to the apoptotic pathway leading to cell death.

A vast majority of the work on apoptosis targeted radiotracers has focused on Annexin V and its derivatives (Fig. 13) [72]. Annexin V is a member of the calcium and phospholipid binding superfamily of Annexin proteins that displays selective, nanomolar affinity ($K_d \sim 0.5$–7 nM) toward phosphatidylserine (PS) residues. Annexin V and its derivatives have been radiolabeled with a wide variety of radionuclides including radioiodine (^{123}I, ^{124}I, ^{125}I), ^{18}F, ^{99m}Tc, ^{111}In, ^{11}C, and ^{64}Cu [73]. Radiolabeled caspase substrates, inhibitors and monoclonal antibodies targeted to human Annexin V have also been reported as alternative approaches for apoptosis imaging [74].

A recent report by Tait and coworkers has compared the apoptosis-specific liver uptake of several ^{99m}Tc-labeled Annexin V derivatives prepared by amine-directed modification with those labeled site-specifically at the N-terminus [75]. A clear improvement was seen for site specific labeling as compared to amine-directed modification. Use of ^{99m}Tc-labeled hydrazinenicotinamide-annexin V imaging for as-
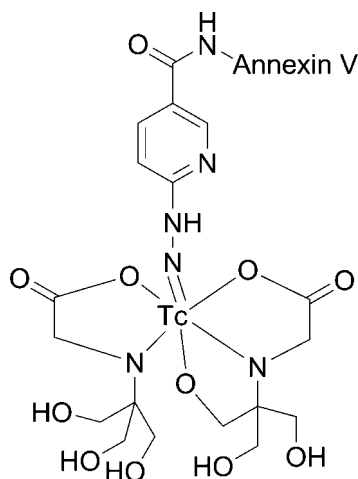
Fig. 13. Structure of ^{99m}Tc-HYNIC annexin V.

sessment of response to chemotherapy has also been reported [76]. The reported imaging protocol was able to distinguish responders from non-responders with 94% accuracy (16/17 patients) and a sensitivity and specificity of 86% and 100%, respectively. ^{99m}Tc-labeled duramycin has proved to have good affinity and selectivity for the PE target [77]. In these studies, ^{99m}Tc-HYNIC-duramycin showed good binding to Jurkat cells induced into apoptosis following camptothecin treatment. This binding could be competitively abolished by the presence of PE containing liposomes, but not by liposomes containing phosphatidylcholine (PC), phosphatidylserine (PS), or phosphatidylglycerol (PG). The results indicate that the binding of ^{99m}Tc-HYNIC-duramycin to the apoptotic cells was exclusively and competitively diminished in the presence of increasing concentrations of PE-containing liposomes, but not by liposomes consisting of PC, PG, or PS.

Continued efforts in the identification of novel molecular targets involved in the apoptotic cascade could contribute to new strategies that would allow early detection of the process by means of specific cell death radiotracers. Furthermore, the therapeutic (*i.e.* apoptosis inhibition) or toxic (*i.e.* apoptosis induction) effect of new drugs can be evaluated by means of specific apoptosis radiotracers. Such markers could also allow physicians to monitor the efficacy of anti-cancer treatment and to select responding from non-responding patients at an early stage of chemotherapy or radiotherapy.

7. Discussion

SPECT has continued to dominate due to lower cost and use of generator-based radionuclides as compared to PET, which required higher infrastructure cost of cyclotron and radiochemistry facilities. In this article, a review of SPECT radiotracers in use and in development has been presented. The applications of SPECT today range from the routine cardiac myocardial perfusion imaging to receptor specific tracers for oncology and neurology. The growth of SPECT however faces its own challenges due to the shortage in supply of ^{99}Mo and ^{99m}Tc arising out of the shutdown of the reactor at Chalk River, which has adversely affected SPECT

users. It has also highlighted the need for SPECT users to adopt alternative radionuclides such as ^{123}I, ^{201}Tl or ^{82}Rb and for manufacturers/suppliers of imaging agents to develop radiotracers with alternative radiotracers. We have described ^{123}I based radiotracers that have been launched in the market and are currently used in Parkinson's disease, cardiology and neurology applications. While ^{123}I requires a cyclotron, it is not currently available outside of US, Europe and Japan and an investment should be made in developing nations to provide this radionuclide as well as alternative radionuclides to drive future radiotracer development for disease areas especially prevalent in developing nations.

In a recent review [78], the four challenges in the field of radiotracer development described were: higher affinity radiotracers, increasing the radiochemical specific activity to reduce competitive binding, supply of ^{99m}Tc and moving radiotracers from research to clinic to market.

Recent advances in chelation chemistry with newer chelators such as the single amino acid chelators that are analogues of lysine [79] and polyester dendrimer [80] that could be labeled with technetium-99m are improving radiotracer kinetics through rapid blood clearance and reduced background. As newer radiotracers are developed that target specific receptors, chelation of ^{99m}Tc into small molecules or peptides still poses challenges in chelator and pharmacophore size, affecting the overall affinity and clearance. In a review of chelators for technetium and gallium radiotracers [81], recommendation was made for a design strategy that takes into account the fundamental coordination chemistry of technetium and factors such as coordination preferences, robust core structures and ligand selection as these are critical to creating effective radiotracers. For SPECT to continue to be the modality of choice, better radiotracer design has to be combined with improvements in hardware to improve image quality.

Valiant [78] also discussed the challenge of taking radiotracers from the bench to the clinic. In this context, it would be important to cite the example of infection imaging which is an unmet need in many developing countries. There have been various attempts to develop agents to image infection using technetium labeled antibiotics, antimicrobial peptides, and even anti-tuberculosis drugs, but none have successfully been launched. The need today is to have the infrastructure, technical expertise and support for systematic pre-clinical evaluations and clinical trials with adequate follow up. This review of advancements in SPECT imaging from hardware/software to new radiotracer development illustrates that SPECT is still very much an attractive modality for current and future disease applications.

References

1. Ryding, E.: SPECT measurements of brain function in dementia; a review. Acta Neurol. Scand. **94**, 54–58 (1996).
2. Pimlott, S. L., Ebemeuer, K. P.: SPECT imaging in dementia. Brit. J. Radiol. **80**, S153–S159 (2007).
3. Valotassiou, V., Wozniak, G., Sifakis, N., Demakopoulos, N., Georgoulias, P.: Radiopharmaceuticals in neurological and psychiatric disorders. Curr. Clin. Pharmacol. **3**, 99–107 (2008).

4. Gambhir, S. S.: Molecular imaging of cancer with positron emission tomography. Nat. Rev. Cancer. **2**, 683–693 (2002).

5. Antoch, G., Vogt, F. M., Freudenberg, L. S., Nazaradeh, F., Goehde, S. C., Barkhausen, J., Dahmen, G., Bockisch, A., Debatin, J. F., Ruehm, S. G.: Whole-body dual-modality PET/CT and whole-body MRI for tumor staging in oncology. J. Am. Med. Ass. **290**, 3199–3206 (2003).

6. Talbot, P. S., Laruelle, M.: The role of *in vivo* molecular imaging with PET and SPECT in the elucidation of psychiatric drug action and new drug development. Eur. Neuropsychopharmacol. **12**, 503–511 (2002).

7. Willmann, J. K., Bruggen, N. V., Dinkelborg, L. M., Gambhir, S. S.: Molecular imaging in drug development. Nat. Rev. Drug Disc. **7**, 591–607 (2008).

8. Chua, S. C., Ganatra, R. H., Green, D. J., Groves, A. M.: Nuclear cardiology: myocardial perfusion imaging with SPECT and PET. Imaging **18**, 166–177 (2006).

9. Kung, M., Zhuang, Z., Hou, C., Kung, H. F.: Development and evaluation of iodinated tracers targeting amyloid plaques for SPECT imaging. J. Mol. Neurosci. **24**, 49–53 (2004).

10. Agdeppa, E. D., Spilker, M. E.: A review of imaging agent development. Am. Ass. of Pharm. Sci. J. **11**, 286–299 (2009).

11. Slomka, P. J., Patton, J. A., Berman, D. S., Germano, G.: Advances in technical aspects of myocardial perfusion SPECT imaging. J. Nucl. Cadiol. **16**, 255–276 (2009).

12. Bybel, B., Brunken, R. C., DiFilippo, F. P., Neumann, D. R., Wu, G., Cerqueira, M. D.: Continuing medical education: SPECT/CT imaging: clinical utility of an emerging technology. Radiographics **28**, 1097–1113 (2008).

13. Zaidi, H., Koral, K. F.: Scatter modelling and compensation in emission tomography. Eur. J. Nucl. Med. Mol. Imaging **31**, 761–782 (2004).

14. Jansen, F. P., Vanderhyden, J.: The future of SPECT in a time of PET. Nucl. Med. Biol. **34**, 733–735 (2007).

15. Klocke, F. J., Baird, M. G., Lorell, B. H., Bateman, T. M., Messer, J. V., Berman, D. S., O'Gara, P. T., Carabello, B. A., Russell Jr., R. O., Cerqueira, M. D., St. John Sutton, M. G., DeMaria, A. N., Udelson, J. E., Kennedy, J. W., Verani, M. S., Williams, K. A.: ACC/AHA/ASNC Guidelines for the Clinical Use of Cardiac Radionuclide Imaging–Executive Summary: a Report of the American College of Cardiology/American Heart Association Task Force on Practice Guidelines (ACC/AHA/ASNC Committee to Revise the 1995 Guidelines for the Clinical Use of Cardiac Radionuclide Imaging). J. Am. Coll. Cardiol. **42**, 1318–1333 (2003).

16. Uematsu, T., Yuen, S., Yukisawa, S., Aramaki, T., Morimoto, N., Endo, M., Furukawa, H., Uchida, Y., Watanabe, J.: Comparison of FDG PET and SPECT for detection of bone metastases in breast cancer. Am. J. Roentgenol. **184**, 1266–1273 (2005).

17. Herholz, K., Schopphoff, H., Schmidt, M., Mielke, R., Eschner, W., Scheidhauer, K., Schicha, H., Heiss, W., Ebmeier. K.: Direct comparison of spatially normalized PET and SPECT scans in Alzheimer's disease. J. Nucl. Med. **43**, 21–26 (2002).

18. Gholamrezanezhad, A., Mirpour, S., Mariani, G.: Future of nuclear medicine: SPECT *vs.* PET. J. Nucl. Med. **50**, 16N–18N (2009).

19. Liu, S., Edwards, D. S.: ^{99m}Tc-labeled small peptides as diagnostic radiopharmaceuticals. Chem. Rev. **99**, 2235–2268 (1999).

20. Jurisson, S. S., Lydon, J. D.: Potential technetium small molecule radiopharmaceuticals. Chem. Rev. **99**, 2205–2218 (1999).

21. Schwochau, K.: *Technetium: Chemistry and Radiopharmaceutical Applications*. 1st Edn., Wiley-VCH, Weinheim (2000).

22. Allen, F. H.: The Cambridge Structural Database: a quarter of a million crystal structures and rising. Acta Cryst. **B58**, 380–388 (2002).

23. Coenen, H. H.: *Radioiodination Reactions for Pharmaceuticals: Compendium for Effective Synthesis Strategies*. Springer, Dordrecht (2006).

24. Mennicke, E., Holschbach, M., Coenen, H. H.: Direct, N. C. A.: electrophilic radioiodination of deactivated arenes with *N*-chlorosuccinimide. J. Label. Compd. Radiopharm. **43**, 721–737 (2000).

25. Chumpradit, S., Kung, M. P., Billings, J., Mach, R., Kung, H. F.: Fluorinated and iodinated dopamine agents: D_2 imaging agents for PET and SPECT. J. Med. Chem. **36**, 221 (1993).

26. Akula, M. R., Zhang, J. H., Kabalka, G. W.: J. Label. Compd. Radiopharm. **44**, s260 (2001).

27. Goodman, M. M., Chen, P., Plisson, C., Martarello, L., Galt, J., Votaw, J. R., Kilts, C. D., Malveaux, G., Camp, V. M., Shi, B., Ely, T. D., Howell, L., McConathy, J., Nemeroff, C. B.: Synthesis and characterization of iodine-123 labeled 2β-carbomethoxy-3β-(4′-((Z)-2-iodoethenyl)phenyl)nortropane. A ligand for *in vivo* imaging of serotonin transporters by single-photon-emission tomography. J. Med. Chem. **46**, 925–935 (2003).

28. Laruelle, M.: Imaging synaptic neurotransmission with *in vivo* binding competition techniques; a critical review. J. Cereb. Blood Flow Metab. **20**, 423–451 (2000).

29. Brooks, D. J.: Positron emission tomography and single photon emission computed tomography in central nervous system drug development. NeuroRx **2**, 226–36 (2005).

30. Agdeppa, E. D., Kepe, V., Liu, J.: Binding characterization of radiofluorinated 6-dialkylamino-2-napthylethylidene derivatives as positron emission tomography imaging probes for β-amyloid plaques in Alzheimer's disease. J. Neurosci. **21**, RC189: 1–5 (2001).

31. Klunk, W. E., Wang, Y., Huang, G.-F.: The binding of 2-(4′-methylaminophenyl)benzothiazole to postmortem brain homogenates is dominated by the amyloid component. J. Neurosci. **23**, 2086–2092 (2003).

32. Seibyl, J., Jennings, D., Koren, A., Skovronsky, D., Tamagnan, G., Marek, K.: Clinical evaluation of [^{123}I] IMPY as a beta-amyloid imaging biomarker in Alzheimer's subjects and controls. J. Nucl. Med. **48**(Suppl. 2), 57P (2007).

33. Kung, H. F., Kung, M.-P., Choi, S. R.: Radiopharmaceuticals for single photon emission computed tomography brain imaging. Semin. Nucl. Med. **33**, 2–13 (2003).

34. Laruelle, M., Abi-Dargham, A., van Dyck, C. H., Rosenblatt, W., Zea-Ponce, Y., Zoghbi, S. S., Baldwin, R. M., Charney, D. S., Hoffer, P. B., Kung, H. F.: SPECT imaging of striatal dopamine release after amphetamine challenge. J. Nucl. Med. **36**, 1182–90 (1995).

35. Klemm, E., Grunwald, F., Kasper, S., Menzel, C., Broich, K., Danos, P., Reichmann, K., Krappel, C., Rieker, O., Briele, B., Hotze, A. L., Moller, H. J., Biersack, H. J.: [^{123}I] IBZM SPECT for imaging of striatal D_2 dopamine receptors in 56 schizophrenic patients taking various neuroleptics. Am. J. Psychiatry **153**, 183–190 (1996).

36. Kauppinen, T., Bergstorm, K., Heikman, P.: Biodistribution and radiation dosimetry of [^{123}I] ADAM in healthy human subjects: preliminary results. Eur. J. Nucl. Med. **30**, 132–136 (2003).

37. Versijpt, J. Dumont, F., Thierens, H., Jansen, H., De Vos, F., Slegers, G., Santens, P., Dierckx, R. A., Korf, J.: Biodistribution and dosimetry of [^{123}I] PK 11195: a potential agent for SPECT imaging of the peripheral benzodiazepine receptor. Eur. J. Nucl. Med. **27**, 1326–1333 (2000).

38. Jain, D.: Technetium-99m labeled myocardial perfusion imaging agents. Semin. Nucl. Med. **29**, 221–236 (1999).

39. Beller, G. A.: Perfusion imaging. J. Am. Coll. Cardiol. **35** (Suppl. B), 29B–31B (2000).

40. Higley, B., Smith, F. W., Smith, T., Gemmell, H. G., Das Gupta, P., Gvozdanovic, D. V., Graham, D., Hinge, D., Davidson, J., Lahiri, A.: Technetium-99m-1,2-bis[bis(2-ethoxyethyl)phosphino]ethane: human biodistribution, dosimetry and safety of a new myocardial perfusion imaging agent. J. Nucl. Med. **34**, 30–38 (1993).

41. Munch, G., Neverve, J., Matsunari, I., Schroter, G., Schwaiger, M.: Myocardial technetium-99m-tetrofosmin and technetium-99m-sestambi kinetics in normal subjects and patients with coronary artery disease. J. Nucl. Med. **38**, 428–432 (1997).

42. Giammarile, F., Lumbroso, J., Ricard, M., Aubert, B., Hartmann, O., Schlumberger, M., Parmentier, C.: Radioiodinated methaiodobenzylguanidine in neuroblastoma: influence of high dose on tumor site detection. Eur. J. Nucl. Med. **13**, 515–522, (1998).

43. Rufini V, Shulkin, B.: The evolution in the use of MIBG in more than 25 years of experimental and clinical applications. Q. J. Nucl. Med. Mol. Imaging **52**, 341–350 (2008).

44. Agostini, D., Verberne, H. J., Hamon, A.: Cardiac [^{123}I]-MIBG scintigraphy in heart failure. Q. J. Nucl. Med. Mol. Imaging **52**, 369–377 (2008).

45. Carrio, I., Cowie, M, R., Yamazaki, J., Udelson, J., Camici, P. G.: Cardiac sympathetic imaging with MIBG in heart failure. J. Am. Coll. Cardiol. **3**, 92–100 (2010).

46. Strauss, H. W., Johnson, M. N., Schoder, H., Tamaki, N.: Meta-iodobenzylguanidine imaging comes of age: A new arrow in the prognostic quiver for heart failure Patients. J. Am. Coll Cardiol. **55**, 2222–2224 (2010).

47. Verberne, H. J., Brewster, L. M., Somsen, G. A., van Eck-Smit, B. L. F.: Prognostic value of myocardial ^{123}I-metaiodobenzyl-guanidine (MIBG) parameters in patients with heart failure: a systematic review. Eur. Heart J. **29**, 1147–1159 (2008).

48. Wiersma, J. J., Verberne, H. J., ten Holt, W. L., Radder, I. M., Dijksman, L. M., van Eck-Smit, B. L. Prognostic value of myocardial [^{123}I]-metaiodobenzylguanidine (MIBG) parameters in patients with heart failure: a systematic review. Eur. Heart J. **29**, 1147–1159 (2008).

49. Jacobson, A. F., Senior, R., Cerqueira, M. D., Wong, N. D., Thomas, G. S., Lopez, V. A., Agostini, D., Weiland, F., Chandna, H., Narula, J.: Myocardial iodine-123 *meta*-iodobenzylguanidine imaging and cardiac events in heart failure. J. Am. Coll. Cardiol. **55**, 2212–2221 (2010).

50. Agostini, D., Carrio, I., Verberne, H. J. How to use myocardial ^{123}I-MIBG scintigraphy in chronic heart failure. Eur. J. Nucl. Med. Mol. Imaging **36**, 555–559 (2009).

51. Shields, A. F.: Positron emission tomography measurement of tumor metabolism and growth: its expanding role in oncology. Mol. Imaging Biol. **8**, 141–150 (2006).

52. Metser, U., Even-Sapir, E. Semin.: Increased ^{18}F-fluorodeoxy-glucose uptake in benign, nonphysiologic lesions found on whole-body positron emission tomography/computed tomography (PET/CT): accumulated data from four years of experience with PET/CT. J. Nucl. Med. **37**, 206–222 (2007).

53. Carmeliet, P.: Angiogenesis in health and disease. Nat. Med. **9**, 653–660 (2003).

54. Sturk, C., Dumont, D.: Angionesis. Chapt. 12, *The Basic Science of Oncology*. (Tannock, I. F., Hill, R,P., Bristow, R. G., Harrington, L., eds.) McGraw-Hill, Medical Pub. Division, New York (2005), pp. 231–248.

55. Bergers, G., Benjamin, L. E.: Tumorigenesis and the angiogenic switch. Nat. Rev. Cancer **3**, 401–410 (2003)

56. Ferrara, N.: The role of VEGF in the regulation of physiological and pathological angiogenesis. Endocr. Rev. **25**, 581–611 (2004).

57. Hicklin, D. J., Ellis, L. M., Role of the vascular endothelial growth factor pathway in tumor growth and angiogenesis. J. Clin. Oncol. **23**, 1011–1027 (2005).

58. Cai, W., Chen, K,, Mohamedali, K. A., Cao, Q., Gambhir, S. S., Rosenblum, M. G., Chen, X.: PET of vascular endothelial growth factor receptor expression. J. Nucl. Med. **47**, 2048–2056 (2006).

59. Chan, C., Sandhu, J., Guha, A., Scollard, D. A., Wang, J., Chen, P., Bai, K., Lee, L., Reilly, R. M. : A human transferrin-vascular endothelial growth factor (hnTf-VEGF) fusion protein containing an integrated binding site for ^{111}In for imaging tumor angiogenesis. J. Nucl. Med. **46**, 1745–1752 (2005).

60. Danen, E. H.: Integrins: regulators of tissue function and cancer progression. Curr. Pharm. Des. **11**, 881–891 (2005)

61. Hood, J. D., Cheresh, D. A.: Role of integrins in cell invasion and migration. Nat. Rev. Cancer **2**, 91–100 (2002).

62. Kumar, C. C.: Integrin $\alpha_v\beta_3$ as a therapeutic target for blocking tumor-induced angiogenesis. Curr. Drug Targets **4**, 123–131 (2003).

63. Ruoslahti, E.: Specialization of tumor vasculature. Nat. Rev. Cancer **2**, 83–90 (2002).

64. Cai, W., Wu, Y,, Chen, K., Cao, Q., Tice, D. A., Chen, X.: *In vitro* and *in vivo* characterization of ^{64}Cu-labeled Abegrin, a humanized monoclonal antibody against integrin $\alpha v\beta$3. Cancer Res. **66**, 9673–9681 (2006).

65. Chen, X.: Integrin $\alpha_v\beta_3$-targeted imaging of lung cancer. Mini. Rev. Med. Chem. **6**, 227–234(2006).

66. Wu, Y., Zhang, X., Xiong, Z., Cheng, Z., Fisher, D. R., Liu, S., Gambhir, S. S., Chen, X.: MicroPET imaging of glioma integrin $\alpha v\beta$3 expression using ^{64}Cu-labeled tetrameric RGD peptide. J. Nucl. Med. **46**, 1707–1718 (2005).

67. Bach-Gansmo, T., Skretting, A., Bogsrud, T. V.: Integrin scinti-mammography using a dedicated breast imaging, solid-state c-camera and ^{99m}Tc-labelled NC100692. Clin. Phys. Funct. Imaging **28**, 235–9 (2008).

68. Bach-Gansmo, T., Danielsson, R., Saracco, A., Wilczek, B., Bogsrud, T., Fangberget, A.: Integrin receptor imaging of breast cancer: A proof-of-concept study to evaluate ^{99m}Tc-NC100692. J. Nucl. Med. **47**, 1434–1439 (2006).

69. Hengartner, M. O.: The biochemistry of apoptosis. Nature **407**, 770–776 (2000).

70. Sims, P. J., Wiedmer, T.: Unraveling the mysteries of phospholipid scrambling. Thromb. Haemost. **86**, 266–275 (2001).

71. Fadeel, B., Xue, D.: The ins and outs of phospholipid asymmetry in the plasma membrane: roles in health and disease. Crit. Rev. Biochem. Mol. Biol. **44**, 264–277 (2009).

72. Blankenberg, F. G.: Recent advances in the imaging of programmed cell death. Curr. Pharm. Des. **10**, 1457–1467 (2004).

73. Lahorte, C. M., Vanderheyden, J. L., Steinmetz, N., Van de Wiele, C., Dierckx, R. A., Slegers, G.: Apoptosis-detecting radioligands: current state of the art and future perspectives. Eur. J. Nucl. Med. Mol. Imaging **31**, 887–919 (2004).

74. Bauer, C., Bauder-Wuest, U., Mier, W., Haberkorn, U., Eisenhut, M.: ^{131}I-labeled peptides as caspase substrates for apoptosis imaging. J. Nucl. Med. **46**, 1066–1074 (2005).

75. Tait, J. F., Smith, C., Levashova, Z., Patel, B., Blankenberg, F. G., Vanderheyden, J. L.: Improved detection of cell death *in vivo* with annexin V radiolabeled by site-specific methods. J. Nucl. Med. **47**, 1546–1553 (2006).

76. Rottey, S., Slegers, G., Van Belle, S., Goethals, I., Van de Wiele, C.: Sequential ^{99m}Tc-hydrazinonicotinamide-annexin V imaging for predicting response to chemotherapy. J. Nucl. Med. **47**, 1813–1818 (2006).

77. Zhao, M., Li, Z., Bugenhagen, S.: ^{99m}Tc-labeled duramycin as a novel phosphatidylethanolamine-binding molecular probe. J. Nucl. Med. **49**, 1345–1352 (2008).

78. Valiant, J. F.: A bridge not too far: Linking disciplines through molecular imaging probes. J. Nucl. Med. **51**, 1258–1268 (2010).

79. Maresca, K. P., Hillier, S. M., Femia, F. J., Zimmerman, C. N., Levadala, M. K., Banerjee, S. R., Hicks, J., Sundararajan, C., Valliant, J., Zubieta, J., Eckelman, W. C., Loyal, J. L., Babich, J. W.: Comprehensive radiolabeling, stability, and tissue distribution studies of technetium-99m single amino acid chelates (SAAC). Bioconjug. Chem. **20**, 1625–1633 (2009).

80. Parrott, M. C., Benhabbour, S. R., Saab, C., Lemon, J. A., Parker, S., Valliant, J. F., Adronov, A.: Synthesis, radiolabeling, and bio-imaging of high-generation polyester dendrimers. J. Am. Chem. Soc. **131**, 2906–2916 (2009).

81. Bartholomä, M. D., Louie, A. S., Valliant, J. F., Zubieta, J.: Technetium and gallium derived radiopharmaceuticals: comparing and contrasting the chemistry of two important radiometals for the molecular imaging era. Chem. Rev. **110**, 2903–2920 (2010).